A New Look at the Discrete Ordinate Method for Radiative Transfer Calculations in Anisotropically Scattering Atmospheres. II: Intensity Computations

KNUT STAMNES AND HENRI DALE[1]

Geophysical Institute, University of Alaska, Fairbanks 99701

(Manuscript received 17 March 1981, in final form 20 July 1981)

ABSTRACT

The recently developed matrix method to solve the discrete ordinate approximation to the radiative transfer equation in plane parallel geometry (Stamnes and Swanson, 1981) is extended to compute the full azimuthal dependence of the intensity. Comparing computed intensities with those obtained by other established methods, we find that for phase functions typical of atmospheric haze 32 streams are sufficient for better than 1% agreement, while 16 streams yield an accuracy of about 1–5% except for angles close to the forward and backward directions for which the error is about 10–15%. The results of the intensity computations are summarized by presenting three-dimensional "stack plots" of the intensity as a function of polar and azimuthal angles. We also show that for flux calculations four streams suffice to obtain 1% accuracy, while eight streams yield an accuracy better than 0.1%.

1. Introduction

In a recent paper (Stamnes and Swanson, 1981) a matrix formulation of the discrete ordinate method was developed for solving the radiative transfer equation in plane parallel geometry. The numerical documentation of the method was restricted to vertical fluxes emerging from the boundaries of a scattering and absorbing medium. For calculations of vertical fluxes, only the azimuth-independent term contributes. Simple expressions for the emergent fluxes were derived by appealing to the reciprocity principle and were used to compute albedo and transmissivity for a parallel beam of radiation incident on a homogeneous slab [cf. Eqs. (34) and (35) of Stamnes and Swanson, 1981].

Although in our previous paper the theoretical analysis and numerical results and comparisons with previous work were given only for the azimuth-independent case (the zero-order Fourier component of the intensity), it was emphasized that the matrix method developed applies equally well to the azimuth-dependent terms. In the present paper we extend the matrix method to compute the complete azimuth dependence of the intensity for a homogeneous, plane parallel, anisotropically scattering atmosphere. Such calculations are pertinent to sky brightness studies. Furthermore, solar energy feasibility studies have shown that radiant energy is most efficiently received by solar collectors which are oriented at certain optimum tilt angles (other than zero) with respect to the horizontal. In order to compute the flux intercepted by such tilted solar receivers the full azimuthal dependence of the sky radiation is required (Dave and Braslau, 1976).

The primary purpose of the present paper, however, is to provide numerical documentation of our method by comparing computed intensities with those obtained by other methods.

2. Theory

The mth Fourier component of the equation describing the transfer of diffuse, monochromatic solar radiation through a plane parallel, homogeneous atmosphere is given by (Chandrasekhar, 1960; Stamnes and Dale, 1981).

$$\mu \frac{dI^m(\tau, \mu)}{d\tau} = I^m(\tau, \mu) - J^m(\tau, \mu), \quad (1)$$

where $J^m(\tau, \mu)$ is the "source function" (cf. Stamnes and Dale, 1981; Stamnes and Swanson, 1981).

Once the intensity components (i.e., the Fourier expansion coefficients), $I^m(\tau, \mu)$, have been determined by solving (1) (for each m) the intensity is given by

$$I(\tau, \mu, \phi) = \sum_{m=0}^{2n-1} I^m(\tau, \mu) \cos m(\phi_0 - \phi). \quad (2)$$

The discrete ordinate approximation to (1) is (cf. Stamnes and Swanson, 1981; Stamnes and Dale, 1981)

[1] Present affiliation: Department of Physics, University of Washington, Seattle 98195.

0022-4928/81/122696-11$06.75

$$\mu_i \frac{dI^m(\tau, \mu_i)}{d\tau} = I^m(\tau, \mu_i) - J^m(\tau, \mu_i). \quad (3)$$

A solution to (3) is obtained by the matrix method developed by Stamnes and Swanson (1981). Thus, the general solution can be written

$$I^m(\tau, \mu_i) = \sum_{j=-n}^{n} L_j^m g_j^m(\mu_i) \exp(-k_j^m \tau) + Z_0^m(\mu_i) \exp(-\tau/\mu_0), \quad (4)$$

where the L_j^m's are constants of integration to be determined from the boundary conditions. The g^m's and k^m's are the solution of an algebraic eigenvalue problem and $Z_0^m(\mu_i)$ values are determined from a system of linear algebraic equations (for details see Stamnes and Dale, 1981; Stamnes and Swanson, 1981).

Proceeding as in Stamnes and Swanson (1981) one finds that the source function, $J^m(\tau, \mu)$, and the angular distribution of the intensity components, $I^m(\tau, \pm\mu)$, are given by (for details see Stamnes and Dale, 1981)

$$J^m(\tau, \mu) = \sum_{j=-n}^{n} (1 + k_j^m \mu) L_j^m g_j^m(\mu) \exp(-k_j^m \tau) + (1 + \mu/\mu_0) Z_0^m(\mu) \exp(-\tau/\mu_0) \quad (5)$$

$$I^m(\tau, +\mu) = \sum_{j=-n}^{n} L_j^m g_j^m(\mu) \times \left\{ \exp(-k_j^m \tau) - \exp\left[k_j^m \tau^* + \frac{1}{\mu} (\tau^* - \tau) \right] \right\} + Z_0^m(\mu) \left\{ \exp(-\tau/\mu_0) - \exp\left[-\tau^*/\mu_0 - \frac{1}{\mu} (\tau^* - \tau) \right] \right\} \quad (6)$$

$$I^m(\tau, -\mu) = \sum_{j=-n}^{n} L_j^m g_j^m(-\mu) \{ \exp(-k_j^m \tau) - \exp(-\tau/\mu) \} \times Z_0^m(-\mu) \{ \exp(-\tau/\mu_0) - \exp(-\tau/\mu) \}. \quad (7)$$

In (6) τ^* is the optical thickness of the plane parallel atmosphere. For $\mu = 0$ we use the expression $I^m(\tau, 0) = J^m(\tau, 0)$ [with $J^m(\tau, 0)$ computed from (5)] which is valid in the limit as μ approaches zero.

Simple expressions for $g_j^m(\mu)$ and $Z_0^m(\mu)$ derivable from (1) are (Stamnes and Dale, 1981)

$$g_i^m(\mu) = \frac{\omega_0}{1 + k_i^m \mu} \sum_{l=m}^{2n-1} (2l + 1) g_l^m P_l^m(\mu) \frac{1}{2} \times \sum_{j=-n}^{n} a_j P_l^m(\mu_j) g_i^m(\mu_j). \quad (8)$$

$$Z_0^m(\mu) = \frac{\omega_0}{1 + \mu/\mu_0} \sum_{l=m}^{2n-1} (2l + 1) g_l^m P_l^m(\mu) \times \left[\frac{1}{2} \sum_{j=-n}^{n} a_j P_l^m(\mu_j) Z_0^m(\mu_j) + \frac{I_{\text{inc}}}{4\pi} (-1)^{l+m} (2 - \delta_{0,m}) P_l^m(\mu_0) \right]. \quad (9)$$

Eqs. (8) and (9) are simply convenient analytic interpolation formulas for the $g_i^m(\mu)$'s and the $Z_0^m(\mu)$'s. The fact that they are obtained from the basic transfer equation (1) to which we are seeking a solution, indicates that these expressions may be superior to any other standard interpolation scheme. A similar interpolation scheme was developed by Fricke (1979), although he did not provide simple expressions for the intensity and source function such as those given by Eqs. (5)–(7).

3. Results and comparisons

The performance and range of validity of any computational method are perhaps best assessed by comparing numerical results with those obtained by other established methods for a variety of conditions. An extensive intercomparison of existing methods for the solution of radiative transfer problems was recently published in a report initiated by the Radiation Commission of the International Association of Meteorology and Atmospheric Physics and edited by Lenoble (cf. Lenoble, 1977; hereafter referred to as "Standard Procedures"). In order to document our method we shall rely heavily on the "benchmark" results provided in "Standard Procedures". Although there are numerous papers on the discrete ordinate method, we know of only one previous paper (Fricke, 1979) in which results for azimuth-dependent terms have been reported. We will compare our discrete ordinate approach with that of Fricke (1979) both with regard to computational procedures and numerical results.

a. Comparison with results provided in "Standard Procedures"

As already mentioned, in our previous paper (Stamnes and Swanson, 1981) we gave results only for albedo and transmissivity due to parallel incident illumination. For completeness we show in Table 1 net fluxes at several optical depths for a parallel beam of radiation incident on a plane-parallel layer of haze particles (Haze L, cf. Deirmendjian, 1969) of total optical thickness $\tau^* = 1$ and single-scattering albedo $\omega_0 = 0.9$. The vertical flux of the incident solar beam in direction μ_0 was assumed to be $\mu_0 I_{\text{inc}} = \mu_0 (I_{\text{inc}} = 1)$. The present results are given for 4, 8, 16, 32 and 48 discrete streams. δ-DOM refers to

TABLE 1. Net flux, $F(\tau)$, for single-scattering albedo, $\omega_0 = 0.9$ and "Haze L" phase function in different orders of approximation. Solar zenith angle is 60° (i.e., $\mu_0 = -0.5$). Results are shown for several optical depths within a layer of optical thickness $\tau^* = 1$.

	4-stream		8-stream		16-stream		32-stream		48-stream		"Standard procedures"	
τ	δ-DOM	DOM	δ-DOM	DOM	δ-DOM	DOM	δ-DOM	DOM	δ-DOM	DOM	Spherical harmonics	Doubling
0.0	1.3337	1.3296	1.3457	1.3459	1.3453	1.3453	1.3453	1.3453	1.3453	1.3453	1.3452	1.3453
0.05	1.3139	1.3092	1.3262	1.3265	1.3257	1.3257	1.3257	1.3257	1.3257	1.3257	1.3257	1.3257
0.1	1.2942	1.2883	1.3063	1.3067	1.3058	1.3059	1.3059	1.3059	1.3059	1.3059	1.3058	1.3059
0.2	1.2553	1.2463	1.2667	1.2672	1.2664	1.2664	1.2664	1.2664	1.2664	1.2664	1.2664	1.2664
0.5	1.1466	1.1278	1.1568	1.1573	1.1568	1.1568	1.1568	1.1568	1.1568	1.1568	1.1567	1.1568
0.75	1.0696	1.0461	1.0791	1.0795	1.0791	1.0791	1.0791	1.0791	1.0791	1.0791	1.0791	1.0791
1.0	1.0074	0.9834	1.0159	1.0161	1.0159	1.0159	1.0159	1.0159	1.0159	1.0159	1.0158	1.0159

our discrete ordinate results using Wiscombe's (1977) δ-L representation for the phase function in which a fraction f of the phase function representing the forward-scattering peak is approximated by a Dirac delta-function and the residual, $(1 - f)$, is expanded in Legendre polynomials. DOM designates our discrete ordinate results using an ordinary Legendre polynomial expansion of the phase function. Results obtained by the doubling and spherical harmonics methods are quoted from "Standard Procedures" for comparison.

The error in the four stream approximation is <1% for δ-DOM and <2% for DOM. For eight streams the relative error is $<10^{-3}$. Only for streams less than eight does δ-DOM perform significantly better than DOM for this particular phase function. Similar results for conservative scattering are reported by Stamnes and Dale (1981).

We will now turn our attention to intensity computations. In Table 2 we show the intensity distribution for an overhead sun ($\mu_0 = -1.0$) and for a single-scattering albedo $\omega_0 = 0.9$. Since this case applies to an overhead sun, the intensity is independent of azimuth and only the zero-order Fourier component ($m = 0$) contributes to the sum in (2). The 48-stream results (and in most cases the 32-stream results) agree to within 1% with the "Spherical harmonic" and "Successive scattering" values quoted from

TABLE 2. Intensities in different orders of approximation for an overhead sun but otherwise similar to the situation in Table 1, i.e., Haze L, $\tau^* = 1$, $\mu_0 = -1$, $\omega_0 = 0.9$.

		Discrete ordinates (δ-DOM)				"Standard procedures"	
τ	μ	8-stream	16-stream	32-stream	48-stream	Spherical harmonics	Successive scattering
	1.0	1.5619 −2	2.3581 −2	2.7321 −2	2.7845 −2	2.794 −2	2.831 −2
	0.8	3.1352 −2	3.2026 −2	3.1455 −2	3.1435 −2	3.145 −2	3.166 −2
	0.6	3.4227 −2	3.9514 −2	3.9179 −2	3.9183 −2	3.913 −2	3.935 −2
0	0.4	6.1288 −2	5.2658 −2	5.3561 −2	5.3588 −2	5.347 −2	5.369 −2
	0.2	6.6530 −2	6.8352 −2	6.6985 −2	6.7021 −2	6.691 −2	6.698 −2
	0	3.4694 −2	4.9952 −2	5.1730 −2	5.1775 −2		5.168 −2
	1.0	8.4580 −3	1.1822 −2	1.3460 −2	1.3693 −2	1.374 −2	1.390 −2
	0.8	1.6117 −2	1.6353 −2	1.6098 −2	1.6090 −2	1.610 −2	1.620 −2
	0.6	2.0066 −2	2.2278 −2	2.2121 −2	2.2124 −2	2.210 −2	2.218 −2
	0.4	4.0839 −2	3.6433 −2	3.6880 −2	3.6897 −2	3.683 −2	3.687 −2
	0.2	6.6556 −2	6.7493 −2	6.6712 −2	6.6729 −2	6.668 −2	6.662 −2
0.5	0	8.3730 −2	9.2853 −2	9.3971 −2	9.3993 −2	9.40 −2	9.387 −2
	−0.2	9.4922 −2	9.3078 −2	9.1523 −2	9.1552 −2	9.155 −2	9.153 −2
	−0.4	1.0078 −1	8.6877 −2	8.8273 −2	8.8285 −2	8.834 −2	8.848 −2
	−0.6	9.7773 −2	1.1568 −1	1.1536 −1	1.1531 −1	1.1532 −1	1.157 −1
	−0.8	2.5325 −1	2.4267 −1	2.3843 −1	2.3851 −1	2.3850 −1	2.395 −1
	−1.0	1.1170 0	1.9289 0	2.2205 0	2.2398 0	2.2396 0	2.239 0
	0	7.7672 −2	7.8964 −2	8.0633 −2	7.9911 −2		7.971 −2
	−0.2	1.2769 −1	1.2517 −1	1.2417 −1	1.2417 −1	1.2413 −1	1.247 −1
	−0.4	1.5862 −1	1.4698 −1	1.4820 −1	1.4822 −1	1.4826 −1	1.491 −1
1	−0.6	1.8089 −1	2.0105 −1	2.0072 −1	2.0067 −1	2.0068 −1	2.019 −1
	−0.8	4.0753 −1	3.9155 −1	3.8686 −1	3.8696 −1	3.8694 −1	3.893 −1
	−1.0	1.5759 0	2.5875 0	2.9437 0	2.9672 0	2.9669 0	2.975 0

"Standard Procedures". Sixteen streams are sufficient to obtain an accuracy of ~1–5% except for angles close to the zenith or nadir directions for which the error is ~10–15%. If an error of ~10–20% can be tolerated, 8-stream results are useful except for angles close to the forward and backward directions where errors of about 50 and 30%, respectively, occur. The large error in the forward direction is due to the truncation of the forward-scattering peak of the phase function (cf. Fig. 1).

Results similar to Table 2 are shown in Table 3 for $\omega_0 = 0.9$, $\mu_0 = -0.5$ and $\Delta\phi = \phi_0 - \phi = 0°$ (azimuthal plane of the sun). The intensities were computed from (2) using $2n - 2$ Fourier components, where $2n$ is the number of streams. Results for 16, 32 and 48 streams are shown for DOM as well as δ-DOM. Comparing the intensity values for DOM and δ-DOM we see that for discrete streams equal to or exceeding 32 there are no significant differences, and these values agree within 1% with those quoted from "Standard Procedures". Similar computations for optical depths 0.05, 0.1, 0.2 and 0.75, and for azimuthal angles $\Delta\phi = 90$ and 180° are reported by Stamnes and Dale (1981).

b. *DOM versus δ-DOM*

In order to look more closely at the relative merits of DOM and δ-DOM, we show in Fig. 1 plots of intensity versus cosine of polar angle for three different optical depths and for azimuthal angles $\Delta\phi = 0$, 90, 180°. The solid curve is for 48 streams (46 azimuthal components) and the dashed and dotted-dashed curves are for 16-stream δ-DOM and DOM, respectively. Considering first the case $\Delta\phi = 0°$ (i.e., the azimuthal plane of the sun) we observe that the largest deviation between the 16-stream and the accurate 48-stream results occurs in the forward direction (i.e., for $\mu \approx \mu_0 = -0.5$). The 16-stream approximation underestimates the intensity near the forward direction, but DOM deviates less than δ-DOM. As already noted this behavior is caused by the truncation of the forward scattering peak in δ-DOM. However, for angles not close to the forward direction δ-DOM performs equally as well or better than DOM. This is particularly noted for $\Delta\phi = 180°$ where 16-stream DOM exhibits an oscillatory behavior with appreciable deviations, while δ-DOM yields quite satisfactory results.

c. *Convergence of the Fourier-sum*

Since the computational burden is directly proportional to the number of azimuth components needed to achieve a given accuracy, it is of great interest to find out how fast the sum in (2) converges. Thus, in Fig. 2 we show for a 48-stream computation the intensity given by (2) versus number of terms included in the sum for $\Delta\phi = 0°$, several values of the polar angle and at three different levels, $\tau = 0.05, 0.5, 0.75$. We note that for angles away from the forward direction ($\mu = -0.1, +0.2, +0.5, +0.8$) less than 10 terms are needed for convergence, whereas about 20 terms are needed for angles close to the forward direction ($\mu = -0.7, -0.4$). In Fig. 3 we display results for the same case as in Fig. 2, but for $\Delta\phi = 90°$.

d. *Intensity patterns*

A compact and instructive way of displaying the intensity pattern is by using three-dimensional plots. Thus, Fig. 4 summarizes the results for the "Haze L" case for $\omega_0 = 0.9$ and $\mu = -0.5$. This figure shows "stack plots" of the intensity as a function of polar and azimuthal angles for six different optical depths ranging from $\tau = 0$ through $\tau = 0.75$. The most striking feature observed in these plots is the rapid decrease in intensity with increasing azimuthal angle. We also note that the reflected intensity exhibits limb brightening, while for optical depths ≤ 0.2 two distinct maxima occur, one close to $\theta = 90°$ and another one close to the direction of incidence $\theta \approx \theta_0 = 60°$. For optical depths >0.2 the two peaks combine to yield a single maximum in the forward direction (i.e., $\mu \approx \mu_0$). The magnitude of the peak intensity generally increases and the peak becomes narrower with optical depth. This behavior is a direct consequence of the strongly forward-peaked phase function associated with "Haze L".

e. *Comparison with Fricke (1979)*

There are basically three ways in which our computational procedures differ from those of Fricke (1979). First, for highly-peaked phase functions Fricke introduces a "phase-integral method" in which the associated Legendre polynomial evaluated at the quadrature point μ_j is replaced by an integration of $P_l^m(\mu)$ over an interval surrounding μ_j, while we have adopted Wiscombe's (1977) method appropriate for highly forward-peaked phase functions.

Second, Fricke also introduces a composite quadrature which consists of dividing the interval $0° < \theta < 90°$ into a number of subintervals bunched near 90°. Within each subinterval he uses a two-point Gaussian quadrature scheme. We use the quadrature rule suggested by Sykes (1951) in which the Gaussian formula is applied separately to the half ranges $-1 < \mu < 0$ and $0 < \mu < 1$. The main advantage of this "double-Gauss" scheme is that the quadrature points are distributed symmetrically around $|\mu| = 0.5$ (in even orders) and bunched both towards $|\mu| = 1$ and $|\mu| = 0$, whereas in the Gaussian scheme for the complete range, $-1 < \mu < 1$, they are bunched toward $|\mu| = 1$. The bunching toward

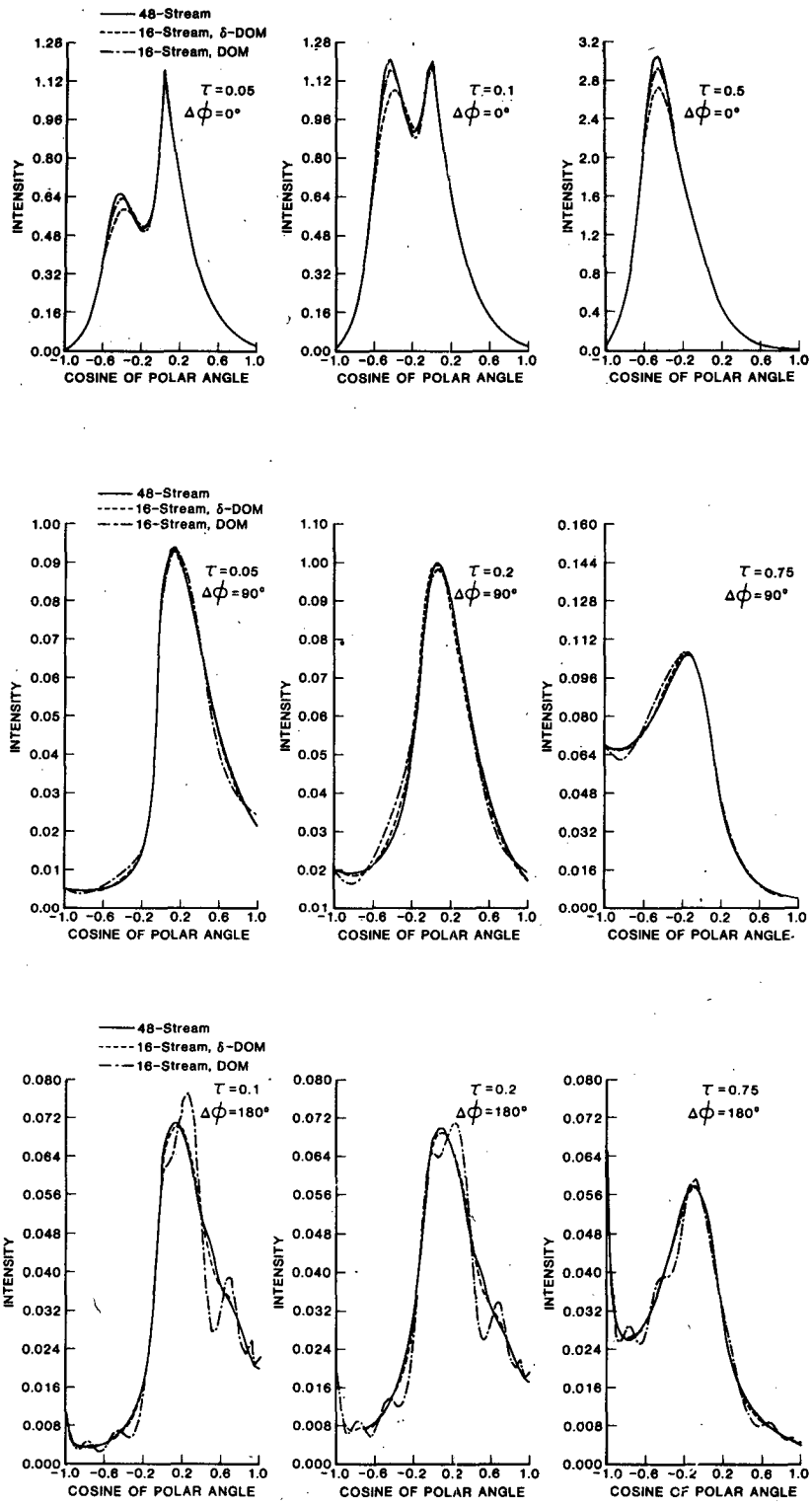

FIG. 1. Comparison of 16-stream DOM and δ-DOM diffuse intensity computations with accurate 48-stream results at several optical depths within a layer of optical thickness $\tau^* = 1$ for $\Delta\phi = 0$, 90 and 180°. "Hase L" with $\omega_0 = 0.9$, $\mu_0 = -0.5$. Note that the ordinate scale is not the same for the various diagrams.

TABLE 3. As in Table 2 except for $\mu_0 = -0.5$ and $\Delta\phi = 0°$ (i.e., azimuthal plane of the sun).

		16-stream		32-stream		48-stream		"Standard procedures"	
								Spherical	Successive
τ	μ	δ-DOM	DOM	δ-DOM	DOM	δ-DOM	DOM	harmonics	scattering
0	1.0	0.23139 −1	0.25879 −1	0.22869 −1	0.22846 −1	0.22856 −1	0.22856 −1	0.2281 −1	0.2278 −1
	0.8	0.65424 −1	0.63712 −1	0.64992 −1	0.65114 −1	0.64984 −1	0.64983 −1	0.6500 −1	0.6462 −1
	0.6	0.14978 +0	0.14509 +0	0.15094 +0	0.15077 +0	0.15096 +0	0.15096 +0	0.1510 +0	0.1501 +0
	0.4	0.33054 +0	0.34271 +0	0.32937 +0	0.32914 +0	0.32932 +0	0.32932 +0	0.3292 +0	0.3274 +0
	0.2	0.65760 +0	0.64167 +0	0.65704 +0	0.65682 +0	0.65686 +0	0.65686 +0	0.6564 +0	0.6522 +0
	0.0	0.10278 +1	0.10580 +1	0.10325 +1	0.10320 +1	0.10319 +1	0.10319 +1		0.1030 +1
0.5	1.0	0.94502 −2	0.10278 −1	0.93682 −2	0.93611 −2	0.93645 −2	0.93645 −2	0.9344 −2	0.9340 −2
	0.8	0.26734 −1	0.26196 −1	0.26605 −1	0.26643 −1	0.26604 −1	0.26604 −1	0.2661 −1	0.2650 −1
	0.6	0.67733 −1	0.66271 −1	0.68097 −1	0.68043 −1	0.68109 −1	0.68109 −1	0.6811 −1	0.6784 −1
	0.4	0.17560 +0	0.17957 +0	0.17523 +0	0.17515 +0	0.17521 +0	0.17521 +0	0.1752 +0	0.1745 +0
	0.2	0.45176 +0	0.44598 +0	0.45157 +0	0.45149 +0	0.45150 +0	0.45150 +0	0.4514 +0	0.4501 +0
	0.0	0.10050 +1	0.10176 +1	0.10090 +1	0.10089 +1	0.10088 +1	0.10088 +1	0.1009 +1	0.1008 +1
	−0.2	0.18428 +1	0.17997 +1	0.18272 +1	0.18270 +1	0.18265 +1	0.18265 +1	0.1826 +1	0.1825 +1
	−0.4	0.27004 +1	0.28568 +1	0.28738 +1	0.28750 +1	0.28728 +1	0.28728 +1	0.2873 +1	0.2862 +1
	−0.6	0.20625 +1	0.21840 +1	0.21857 +1	0.21856 +1	0.21840 +1	0.21840 +1	0.2184 +1	0.2178 +1
	−0.8	0.56357 +0	0.55465 +0	0.56948 +0	0.56929 +0	0.56966 +0	0.56966 +0	0.5696 +0	0.5705 +0
	−1.0	0.48411 −1	0.47370 −1	0.47586 −1	0.47695 −1	0.47590 −1	0.47590 −1	0.4760 −1	0.4772 −1
1.0	0.0	0.52467 +0	0.52725 +0	0.53185 +0	0.53177 +0	0.52772 +0	0.52772 +0		0.5231 +0
	−0.2	0.12990 +1	0.12797 +1	0.12919 +1	0.12919 +1	0.12916 +1	0.12916 +1	0.1291 +1	0.1289 +1
	−0.4	0.22872 +1	0.23899 +1	0.24015 +1	0.24022 +1	0.24008 +1	0.24008 +1	0.2401 +1	0.2392 +1
	−0.6	0.20558 +1	0.21540 +1	0.21550 +1	0.21550 +1	0.21537 +1	0.21537 +1	0.2153 +1	0.2148 +1
	−0.8	0.71437 +0	0.70604 +0	0.71985 +0	0.71968 +0	0.72002 +0	0.72002 +0	0.7199 +0	0.7206 +0
	−1.0	0.84531 −1	0.83580 −1	0.83730 −1	0.83836 −1	0.83735 −1	0.83735 −1	0.8375 −1	0.8403 −1

$|\mu| = 0$ (a property shared by double Gauss and Fricke's composite quadrature) will give superior results near the boundaries where the intensity varies rapidly around $|\mu| = 0$. A half range scheme is also preferable in this respect since the intensity is discontinuous at the boundaries. Another advantage of a half range scheme such as double Gauss over a full range scheme is that upward and downward fluxes

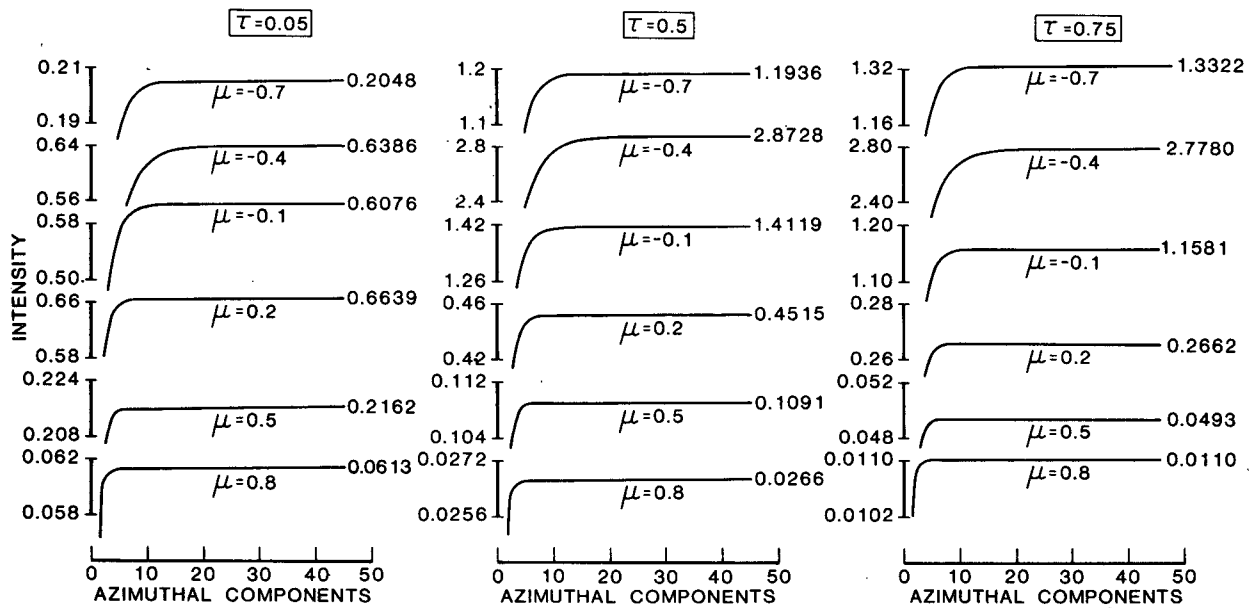

FIG. 2. Diffuse intensity as a function of azimuthal components [i.e., number of terms used in the summation in Eq. (5)] for $\Delta\phi = 0°$, several polar angles and optical depths. "Haze L" with $\omega_0 = 0.9$, $\mu_0 = -0.5$ and $\tau^* = 1$. Note that the ordinate scale is not the same for the various diagrams.

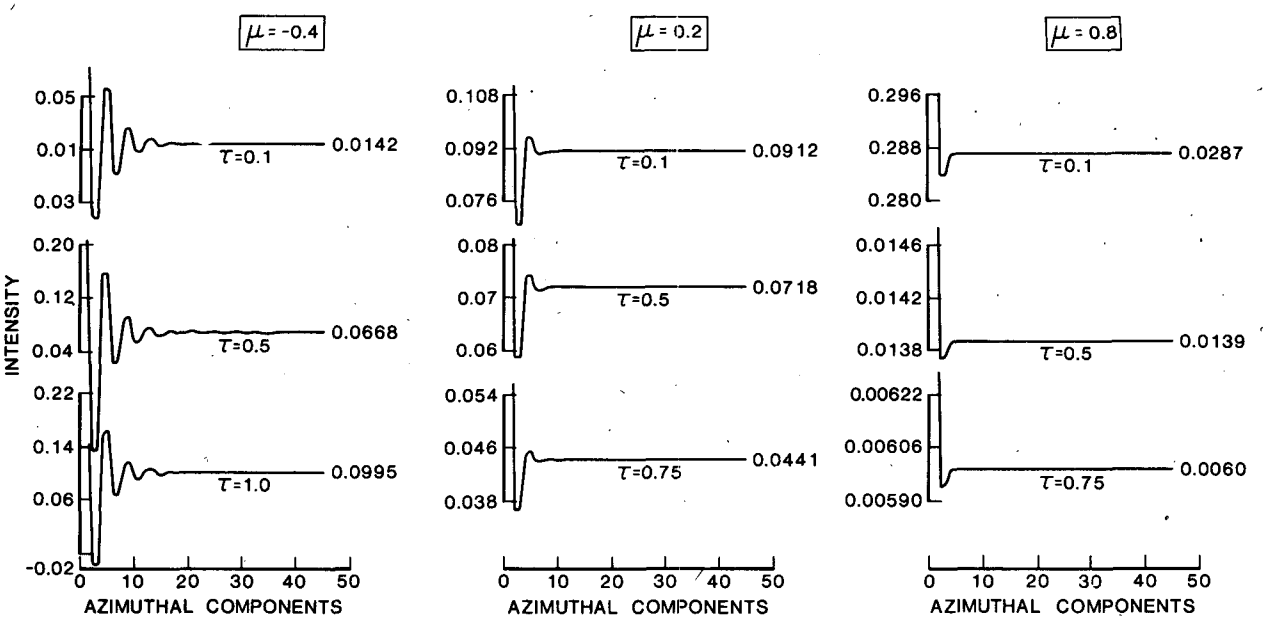

FIG. 3. Similar to Fig. 2 except for $\Delta\phi = 90°$. Note that the ordinate scale is not the same for the various diagrams.

are obtained immediately without any further approximations.

Third, our approach for solving the algebraic eigenvalue problem appears to be quite different from Fricke's. In our previous paper (Stamnes and Swanson, 1981) we showed how the fact that the eigenvalues occur in pairs ($\pm k^m$) can be used to reduce the order of the algebraic eigenvalue problem by a factor of 2. Since the computing time for eigenvalue problems goes as the order of the system cubed, computer time is reduced by a factor of 8. To solve the algebraic eigenvalue problem we use standard, but highly sophisticated routines specifically designed to handle such problems (Stamnes and Swanson, 1981) while Fricke uses a Gauss-Seidel method which he notes to be efficient for large m. It is not clear whether he also uses the same method for small m (including $m = 0$).

Fricke provides numerical results only for the conservative case. In Table 4 we compare our results for transmission and reflection with those reported by Fricke (1979) for $\Delta\phi = 0$ and 90° (similar comparisons for $\Delta\phi = 10$, 40 and 180° are provided by Stamnes and Dale, 1981). These results are for a parallel beam of radiation incident at a polar angle $\theta_0 = 85°$ on a plane-parallel, homogeneous slab of optical thickness $\tau^* = 1$. The incident flux, $\mu_0 I_{\text{inc}}$, was taken to be $\mu_0(I_{\text{inc}} = 1)$. A Henyey-Greenstein phase function with asymmetry factor $g = 0.794$ was used and the single scattering albedo was set to $\omega_0 = 0.99999$ to mimic conservative scattering. Intensities emerging from the top and bottom of the slab are shown for several polar and azimuthal angles. Prior to discussing the results we note that our computations were done on a VAX 11/780 computer using single precision (7-digit) arithmetic, while Fricke used a CDC 6600 computer with 14-digit arithmetic in single precision.

Comparing first our 16-stream results with those of Fricke it is clear that his composite quadrature works better for reflected intensities especially for large polar angles. The composite quadrature is probably designed to give optimal results for reflection at $\theta = 90°$. This conjecture is corroborated by noting that our 16-stream results for transmission are just as accurate as those of Fricke.

Next we note that our 48-stream results are identical to those of Fricke. Thus, we have found no evidence that his composite quadrature gives any improvement as compared to double Gauss for discrete ordinates larger than 16. On the other hand the comparatively poor 48-stream results obtained by Fricke using a full-range Gaussian quadrature (cf. his Fig. 1 which shows an error of 0.3% for Guassian quadrature) demonstrate nicely the computational advantages of using the half range double-Gauss scheme adopted here.

To better visualize the intensity pattern for this case we show in Fig. 5 stack plots (similar to those of Fig. 4) of the intensity as a function of polar and azimuthal angles for several optical depths. We see that at the top of the atmosphere the intensity peaks very sharply at 90°. This strong limb-brightening effect is caused by a combination of large incidence angle ($\theta_0 = 85°$) and forward-peaked scattering. As the optical depth increases the intensity peak

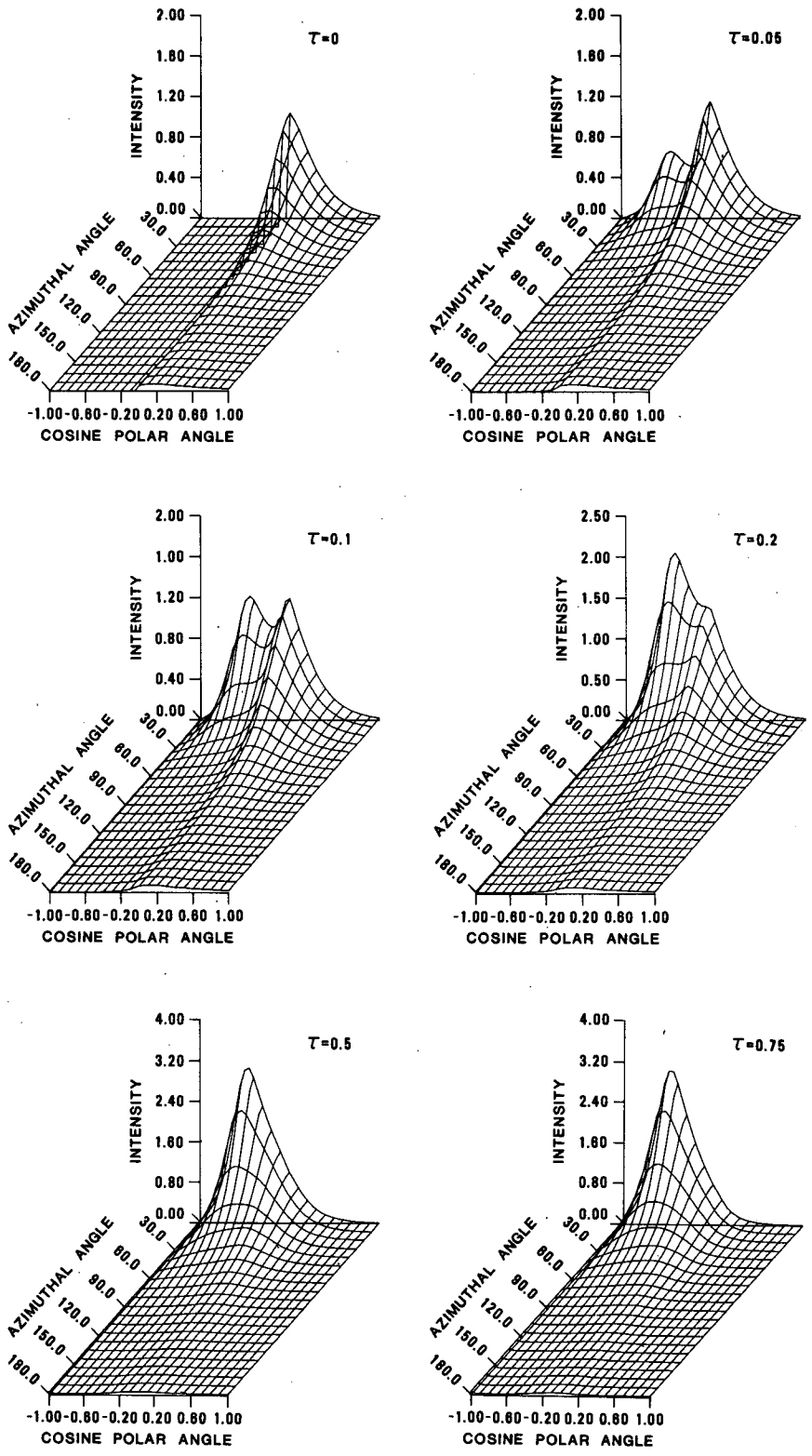

FIG. 4. Three-dimensional "stack plot" of diffuse intensity versus polar and azimuthal angles for several optical depths within a layer of optical thickness $\tau^* = 1$. "Haze L" with $\omega_0 = 0.9$, $\mu_0 = -0.5$. Note that the ordinate scale is not the same for the various diagrams.

TABLE 4. Reflection and transmission for a parallel beam incident at $\theta = 85°$ on a plane parallel slab that scatters according to Henyey-Greenstein phase function with asymmetry factor $g = 0.794$. $2n$ indicates number of streams.

		$\Delta\phi = 0°$								
					$2n = 48$		$2n = 32$		$2n = 16$	
τ	θ	$2n = 16$ Fricke	$2n = 48$ Fricke	$2n = 64$ δ-DOM	δ-DOM	DOM	δ-DOM	DOM	δ-DOM	DOM
	90	9.434	9.4409	9.4410	9.4422	9.4414	9.4124	9.4520	7.8746	8.9072
	88	6.293	6.3050	6.3053	6.3057	6.3050	6.3175	6.3137	5.6123	6.2257
0	85	3.602	3.6052	3.6053	3.6051	3.6053	3.6096	3.5990	3.5052	3.7214
	60	0.173	0.1720	0.1720	0.1720	0.1720	0.1718	0.1718	0.1760	0.1812
	0	0.011	0.0111	0.0111	0.0111	0.0111	0.0111	0.0112	0.0110	0.0123
	90	0.058	0.0581	0.0590	0.0586	0.0586	0.0592	0.0592	0.0587	0.0583
	95	0.102	0.1031	0.1031	0.1031	0.1031	0.1031	0.1032	0.1023	0.1035
1	110	0.263	0.2633	0.2633	0.2633	0.2633	0.2632	0.2633	0.2667	0.2636
	140	0.068	0.0670	0.0670	0.0670	0.0670	0.0670	0.0669	0.0664	0.0647
	180	0.014	0.0160	0.0160	0.0160	0.0160	0.0160	0.0160	0.0160	0.0152
		$\Delta\phi = 90°$								
					$2n = 48$		$2n = 32$		$2n = 16$	
τ	θ	$2n = 16$ Fricke	$2n = 48$ Fricke	$2n = 64$ δ-DOM	δ-DOM	DOM	δ-DOM	DOM	δ-DOM	DOM
	90	0.084	0.0841	0.0841	0.0841	0.0842	0.0850	0.0860	0.1113	0.1417
	88	0.082	0.0824	0.0824	0.0825	0.0825	0.0829	0.0835	0.1001	0.1197
0	85	0.073	0.0732	0.0732	0.0732	0.0732	0.0734	0.0736	0.0839	0.0942
	60	0.028	0.0279	0.0279	0.0279	0.0279	0.0278	0.0279	0.0276	0.0269
	0	0.011	0.0111	0.0111	0.0111	0.0111	0.0111	0.0112	0.0110	0.0123
	90	0.015	0.0146	0.0148	0.0147	0.0147	0.0149	0.0149	0.0147	0.0146
	95	0.022	0.0218	0.0218	0.0218	0.0218	0.0218	0.0218	0.0218	0.0218
1	110	0.030	0.0298	0.0298	0.0298	0.0298	0.0298	0.0298	0.0301	0.0304
	140	0.021	0.0205	0.0205	0.0205	0.0205	0.0205	0.0205	0.0205	0.0195
	180	0.014	0.0160	0.0160	0.0160	0.0160	0.0160	0.0160	0.0160	0.0152

broadens and decreases in magnitude. However, in contrast to the situation shown in Fig. 4 no "double-peak" develops at small optical depth ($\tau < 0.2$). The reason for this is mainly that the angles of incidence are different in the two cases. For the situation in Fig. 5 the angle of incidence is too close to $\theta = 90°$ for two separate peaks to develop. Instead, a single maximum of very high intensity occurs. The magnitude of this peak decreases quite rapidly with optical depth.

4. Summary and conclusions

We have extended the discrete ordinate method of Stamnes and Swanson (1981) to compute the complete azimuthal dependence of the intensity. Such computations are pertinent to sky brightness studies in general, and they are in particular required to compute the flux intercepted by tilted (with respect to the horizontal) solar collectors.

Using our method to compute net vertical fluxes we find that for four streams the error is less than 1% while it is <0.1% for eight streams.

Comparing our computed intensities with those obtained by the "Spherical Harmonic" and the "Successive Scattering" methods we find that 32 streams are sufficient for better than 1% agreement, which is comparable to the agreement between the latter two methods. For the "Haze-L" phase function 16 streams are sufficient to obtain an accuracy of ~1–5% except for angles close to the forward and backward directions for which the error is ~10–15%. We expect these errors to be typical for haze-type phase functions.

An intercomparison of DOM (discrete ordinate method with the usual Legendre polynomial expansion of the phase function) and δ-DOM (discrete ordinate method using Wiscombe's (1977) delta-Legendre representation of the phase function) shows that no significant differences occur for number of streams equal to or exceeding 32 (for Haze-L phase function). For 16 streams, δ-DOM performs equally as well or better than DOM except for angles close to the forward direction.

We also compare our computations with those of

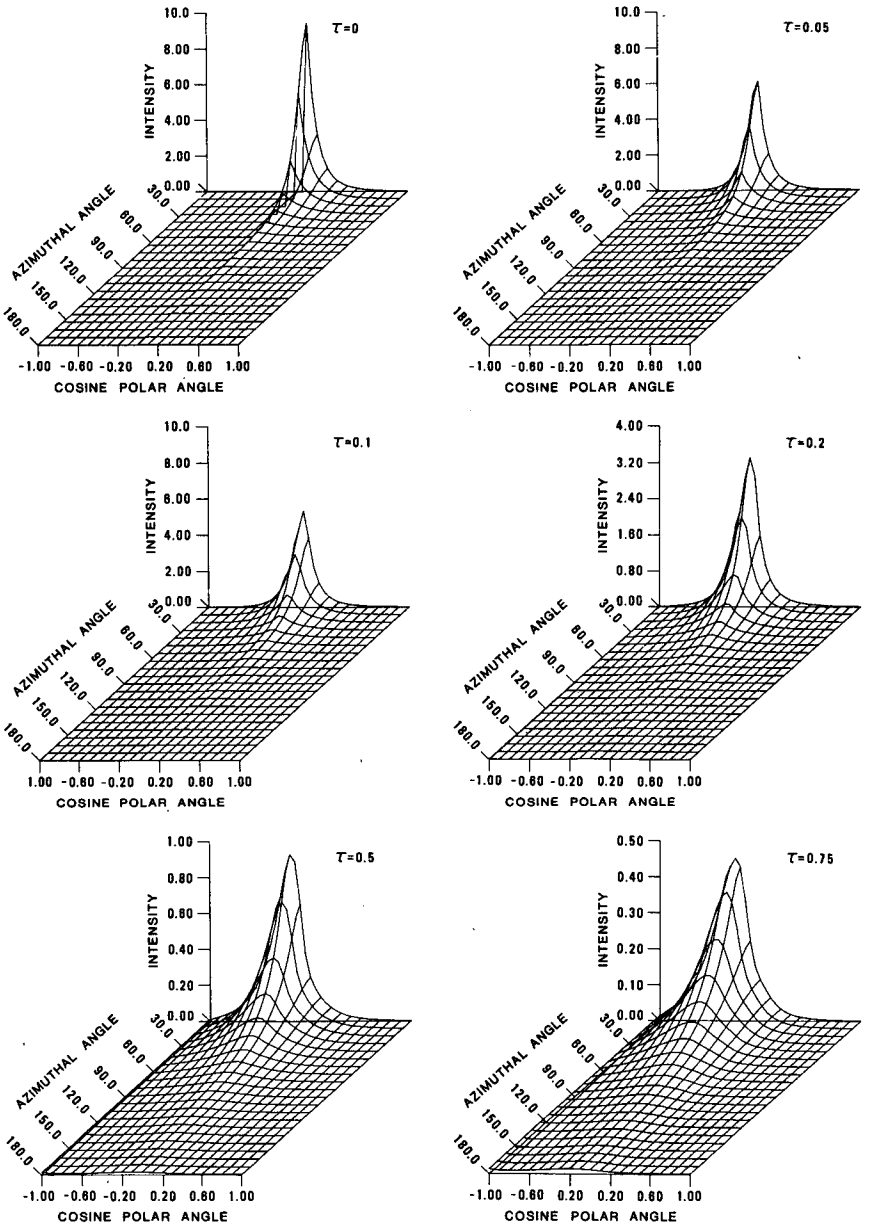

FIG. 5. Similar to Fig. 4 but for Henyey-Greenstein phase function with $g = 0.794$, $\omega_0 = 1$, $\theta_0 = 85°$. Note that the ordinate scale is not the same for the various diagrams.

Fricke (1979) for a Henyey-Greenstein phase function with conservative scattering. Although Fricke also uses a discrete ordinate method his computational procedures differ from ours in that 1) Fricke uses a "composite quadrature" whereas we have adopted a half range Gaussian quadrature (double Gauss); and 2) Fricke uses a Gauss-Seidel method to solve the algebraic eigenvalue problem while we use standard, but highly sophisticated algebraic eigenvalue solvers. Comparing the results we generally find good agreement which implies that Fricke's "composite quadrature" gives essentially no improvement beyond the comparatively much simpler double-Gauss scheme adopted here.

Finally, we present three-dimensional "stack plots" of the intensity as a function of polar and azimuthal angles for several optical depths. Such plots provide a very compact and instructive means of summarizing the results of intensity computations.

Acknowledgments. We greatly appreciate the continued interest, encouragement and support of this

work by M. H. Rees. One of us (K.S.) has also benefited from many helpful discussions with R. A. Swanson. This research was supported by the National Science Foundation through Grants ATM 79-23266 and ATM 79-26406 to the University of Alaska.

REFERENCES

Chandrasekhar, S., 1960: *Radiative Transfer*. Dover, 393 pp.

Deirmendjian, D., 1969: *Electromagnetic Scattering on Spherical Polydispersions*. Elsevier, 290 pp.

Dave, J. V., and N. Braslau, 1976: Importance of the diffuse sky radiation in evaluation of the performance of a solar cell. *Solar Energy*, **18**, 215–223.

Fricke, C. L., 1979: The phase-integral method for radiative transfer problems with highly-peaked phase functions. *J. Quant. Spectrosc. Radiat. Transfer*, **20**, 429–445.

Lenoble, J., Ed., 1977: Standard procedures to compute atmospheric radiative transfer in a scattering atmosphere. Under Auspices of Radiation Commission, Intl. Assoc. Meteor. Atmos. Phys., 123 pp. [Available from Universite des Sciences et Techniques de Lille, U.E.R., de Physique Fondamentale, Laboratoire d'Optique Atmospherique, B.P. 36-59650, Villeneuve d'Ascq, France.]

Stamnes, K., and H. Dale, 1981: On the discrete ordinate method for radiative transfer calculations in anisotropically scattering atmospheres. II. Intensity computations. Sci. Rep., Geophys. Inst., University of Alaska, UAG R-281, 47 pp.

——, and R. A. Swanson, 1981: A new look at the discrete ordinate method for radiative transfer calculations in anisotropically scattering atmospheres. *J. Atmos. Sci.*, **38**, 387–399.

Sykes, J. B., 1951: Approximate integration of the equation of transfer. *Mon. Not. Roy. Astron. Soc.*, **111**, 377–386.

Wiscombe, W. J., 1977: The delta-M method: Rapid yet accurate radiative flux calculations for strongly asymmetric phase functions. *J. Atmos. Sci.*, **34**, 1408–1422.